URSI AP-RASC 2019, New Delhi, India; 09 - 15 March 2019

Space Filling Curves: Heuristics For Semi Classical Lasing Computations

Rohit Goswami[(1)], Amrita Goswami[(1)], and Debabrata Goswami*[(2)]
(1) Department of Chemical Engineering, IIT Kanpur, UP, 208016, India http://iitk.ac.in
(2) Department of Chemistry, IIT Kanpur, UP, 208016, India http://iitk.ac.in

Abstract

For semi classical lasing, the FDTD (finite difference time domain) formulation including nonlinearities is often used. We determine the computational efficiency of such schemes quantitatively and present a hueristic based on space filling curves to minimize complexity. The sparse matrix kernel is shown to be optimized by the utilization of Bi-directional Incremental Compressed Row Storage (BICRS). Extensions to high performance clusters and parallelization are also derived.

1 Introduction

The empirical knowledge of light matter interactions and propogations has been quantified cohesively since the close of the nineteenth century by Maxwell [1]. With the advent of high performance computing (HPC) clusters, methods which were once discarded for their computational excesses show new promise. This surge is evident in the so-called 'brute force' class of computational methods which comprise of the explicit finite difference time domain (FDTD) solvers. This recent interest may be attributed to their fundamental simplicity and generality of application compared to the tailored numerical methods typically employed for specific large system analysis (e.g. nonlinear Schrodinger approximation). The time dependent form of Maxwell's equations for scattering becomes computationally intractable (for the FDTD scheme) as the ratio between the characteristic linear dimension of the object with respect to the wavelength becomes large [2]. The increase in computational cost and poor scaling is offset sharply by the benefit of being able to handle complex geometries and easy source additions. The finite difference time domain technique is thus barred from use on large systems due to poor scaling. Complicating matters, computationally efficient grid methods like adaptive multigrid meshes are not applicable to the solution of these equations for all but low frequency cases due to oscilatory nature of higher frequency systems. The differential solver typically used has been extended to complex lasing systems[3] which show promise for ultrafast pulse interactions. Additionally the numerical solution of systems shown here in this manner forms solutions which are easily compared directly to experimental data. Hence the application of highly efficient data manipulation techniques for HPC software packages is also relevant to the processing of experimental data. Indeed the same data structures may be used to efficiently interpolate numerical and experimental solutions.

We present here, the following numerical schema to efficiently compute the features of interest. The standard constitutive equations are discussed along with the reported update mechanisms, before space filling curves are introduced, along with the necessary data structures for maximally cache oblivous action. Suitable metrics to quantify the bounds of the acceleration described are also derived.

2 Quasi Classical Lasing

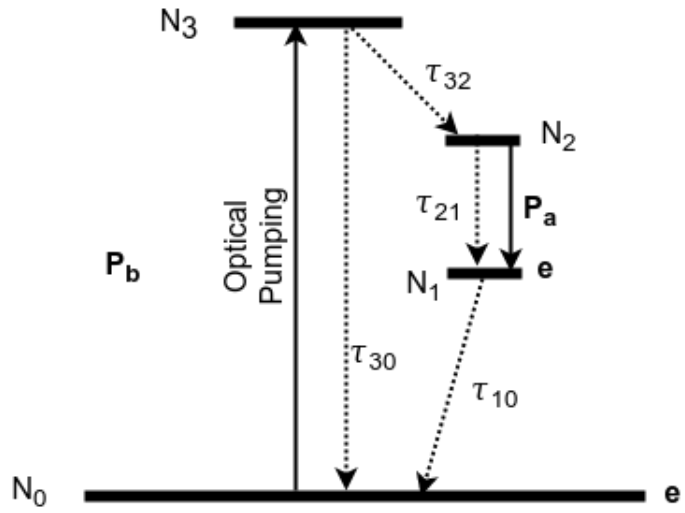

Figure 1. Four level 2 electron model system.

Let us consider the lasing scheme for a four level two electron atomic system [3] shown in Figure 1. For this setup, our constitutive equations are (where P is the polarization density, P_a is the interband photon absorbing and P_b is the interband photon emitting densities):

1. The simplified two level Bloch equations (governing equations):

$$\frac{d^2P_a}{dt^2} + \gamma_a \frac{dP_a}{dt} + \omega_a^2 P_a = \xi_a (N_2 - N_1) E \qquad (1)$$

$$\frac{d^2P_b}{dt^2} + \gamma_b \frac{dP_b}{dt} + \omega_a^2 P_b = \xi_b (N_3 - N_0) E \qquad (2)$$

2. The four level electron populations:

$$\frac{dN_3}{dt} = -\frac{N_3(1-N_2)}{\tau_{32}} - \frac{N_3(1-N_0)}{\tau_{30}} + \frac{1}{\hbar\omega_b}E\cdot\frac{dP_b}{dt} \tag{3}$$

$$\frac{dN_2}{dt} = \frac{N_3(1-N_2)}{\tau_{32}} - \frac{N_2(1-N_1)}{\tau_{21}} + \frac{1}{\hbar\omega_a}E\cdot\frac{dP_a}{dt} \tag{4}$$

$$\frac{dN_1}{dt} = \frac{N_2(1-N_1)}{\tau_{21}} - \frac{N_1(1-N_0)}{\tau_{10}} + \frac{1}{\hbar\omega_a}E\cdot\frac{dP_a}{dt} \tag{5}$$

$$\frac{dN_0}{dt} = \frac{N_3(1-N_0)}{\tau_{30}} - \frac{N_1(1-N_0)}{\tau_{10}} + \frac{1}{\hbar\omega_b}E\cdot\frac{dP_b}{dt} \tag{6}$$

3. These are coupled to the Maxwell-Ampere law:

$$\frac{dE}{dt} = \frac{1}{\varepsilon}\nabla\times H - \frac{1}{\varepsilon}N_{density}\left(\frac{dP_a}{dt} + \frac{dP_b}{dt}\right) \tag{7}$$

4. While to advance the magnetic vector through time, the Maxwell-Faraday law is used:

$$\nabla\times E = -\frac{\delta B}{\delta t} \tag{8}$$

We note that P_i is the polarization density, with the resonant frequency ω, which in turn furnishes $\hbar\omega$ as the energy difference, $\xi_a = 6\pi\varepsilon_0 c^3/\omega_{21}^2\tau_{21}$ and γ_i is the damping coefficient to simulate the nonradiation loss. Finally the electric field is inclusive of the contributions of both pumping and emission signals. We shall discretize the solution in both time and space so as to obtain the characteristic leap-frog schema.

3 Grid Solution Setup

In this case the field update equations are implicitly dependent on the electron populations. Since the derviation of the equations above treats only the atom quantum mechanically, we shall update the time step purely through considerations of Maxwell's equations. No attempt is made here to discuss the numerical instabilities common to all grid solvers. It is expedient to note that higher order difference approximations are typically of limited usage as they do not handle multiple boundaries. We shall also rely on the classical field update limit of the propogation, that is we shall use the Courant number [4], given by $S_c = \frac{c\Delta_t}{\Delta_x}$. Following Chang and Taflove [3] we shall restrict ourselves to the one dimensional case, and therefore take the optimum ratio for the Courant number to be 1. The relevant discretized update equations are then as mentioned shown by [5]:

1. Polarization density update:

$$P_a^{n+1} = C_{a,1}P_a^n + C_{a,2}P_a^{n-1} + C_{a,3}\xi_a(N_2-N_1)E^n \tag{9}$$

Where:

$$C_{a,1} = \frac{2-\omega_a^2(\Delta_t)^2}{1+\gamma_a\Delta_t/2} \tag{10}$$

$$C_{a,2} = \frac{1-\gamma_a\Delta_t/2}{1+\gamma_a\Delta_t/2} \tag{11}$$

$$C_{a,3} = \frac{\Delta_t^2}{1+\gamma_a\Delta_t/2} \tag{12}$$

A similar update is performed for P_b

2. Maxwell-Ampere update (about m)

$$E_z^{n+1}[m] = \frac{\Delta_t}{\Delta_x\varepsilon}(H_y^{n+0.5}[m+0.5] - H_y^{n+0.5}[m-0.5]) - N_{density}\varepsilon[\Delta P_a + \Delta P_b] \tag{13}$$

Where it it understood that $H^{n+0.5}$ is initially specified law, and ΔP_i is the finite time difference of the polarization densities at time levels $n-1$ and $n+1$ to achieve a central difference.

3. Explicit Population Density Update

$$N_3^{n+0.5} = \frac{\tau_{30}\tau_{32}\Delta_t}{2\tau_{30}\tau_{32} + \tau_{30}(1-N_2^n)\Delta_t + \tau_{32}(1-N_0^n)\Delta_t} \left[N_3^{n-0.5}\left(\frac{N_0^n-1}{\tau_{30}} - \frac{N_2^n-1}{\tau_{32}} + \frac{2}{\Delta_t}\right) + \frac{E^n\cdot(P_a^{n+1}-P_a^{n-1})}{\hbar\omega_b\Delta_t}\right] \tag{14}$$

$$N_1^{n+0.5} = \frac{\tau_{10}\tau_{21}\Delta_t}{2\tau_{10}\tau_{21} + \tau_{10}N_2^n\Delta_t + \tau_{21}(1-N_0^n)\Delta_t} \left[N_3^{n-0.5}\left(\frac{N_0^n-1}{\tau_{10}} - \frac{N_2^n}{\tau_{21}} + \frac{2}{\Delta_t}\right) + \frac{2N_2^n}{\tau_{21}} - \frac{E^n\cdot(P_a^{n+1}-P_a^{n-1})}{\hbar\omega_b\Delta_t}\right] \tag{15}$$

$$N_2^{n+0.5} = \frac{\tau_{21}\tau_{32}\Delta_t}{2\tau_{21}\tau_{32} + \tau_{21}N_3^{n+0.5}\Delta_t + \tau_{32}(1-N_1^{n+0.5})\Delta_t} [N_2^n\left(\frac{N_1^{n+0.5}-1}{\tau_{21}} - \frac{N_3^{n+0.5}}{\tau_{32}} + \frac{2}{\Delta_t}\right) + \frac{2N_3^{n+0.5}}{\tau_{32}} + \frac{(E^{n+1}+E^n)\cdot(P_a^{n+1}-P_a^{n-1})}{\hbar\omega_b\Delta_t}] \tag{16}$$

$$N_0 = 1 - N_3 - N_2 - N_1 \tag{17}$$

Where we have simply used the conservation law for the last density.

4. Maxwell-Faraday update (about grid point m)

$$H_y^{n+0.5}[m+0.5] = H_y^{n-0.5} + \frac{\Delta_t}{\mu\Delta_x}(E_z^n[m+1] - E_z^n[m]) \tag{18}$$

Each grid point, apart from the initial conditions (excluding boundary values, Figure 2) of $P_a^n, P_b^n, E^n, H^{n+0.5}, N_1^{n-0.5}, N_0^n$ can be written out in the form of an 'element' equation, and

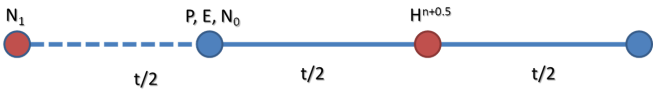

Figure 2. Initial 1D computational scheme.

then assembled over the entire grid as is standard for the 1D finite element methods such as the weak formulation of the Galerkin method [6]. We note that the equations above can be generalized further to a three dimensional N-level atomic system. We shall now enumerate the form of an optimal solver.

4 Operational Optimality

We presume certain ideas of solution optimality, namely, we shall aim for:

- Scalability
- Cache Oblivous Operation

Where scalability shall be assumed to imply a scaling over computational resources either in terms of solver speed or system size. Cache oblivous shall mean that the algorithmic form is able to efficiently use the cache (high cache hit ratio) without consideration of exact CPU architecture. For practical purposes this is possible by the transformation of data to a 1D form, as 1D data structures are cache oblivous. We shall now shift to the usage of space filling curve techniques to solve the system of element equations defined above. First we shall note that for our purposes, it is suitable to define a space filling curve to be a many-to-one dimensional mapping such that locality is preserved. Furthermore, recognizing that the solution to the system defined is essentially the solution of either an equivalent sparse matrix equation, we shall consider the Peano curve (for matrix-matrix multiplication), as well as the Hilbert curve (for matrix-vector operations, parallelization and distribution) [7]. To ensure cache oblivious operation, the Hilbert curve is used to store the nonzeros of the sparse matrix and further we note that the standard form of the 1D Galerkin is of the form amenable to the Bi-directional Incremental CRS (Compressed Row Storage) (BICRS) [8]. This is evident from the sparse matrix vector multiplication which is required for each step's global update. Due to the structured nature of the matrix assembled as part of the Finite Element formulation however, the CRS (Compressed Row Storage) may well be more suitable. For the matrix-vector operations we obtain m^2 operations for $2m$ elements whenever $m \leq n$ and n is the order of the matrix [7]. The Hilbert curve generation via recursion is shown in Figure 3.

We also deal with the overall decomposition of the problem space across processors in terms of the Hilbert curve. Here we utilize the fact that a matrix in memory can be discretized and traversed as an optimal stack [7] (Figure 4).

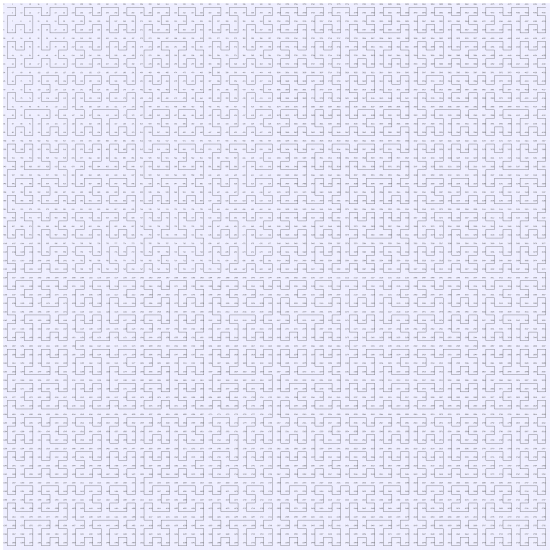

Figure 3. Hilbert curve to and from a 6 by 6 space

The fast fourier transform and its inverse is used to convert the numerical signal obtained into familiar data [3].

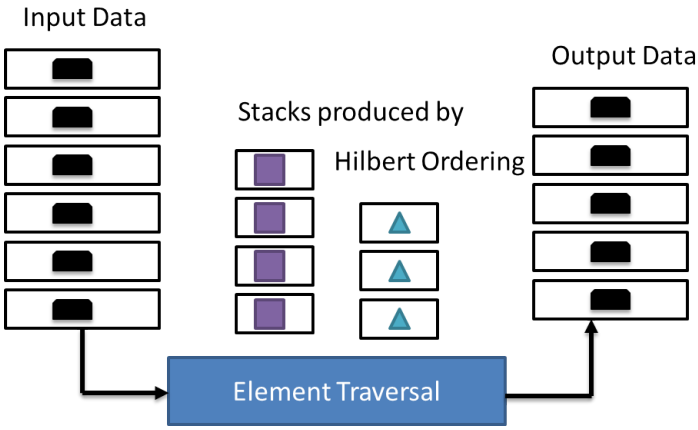

Figure 4. Division and traversal of data stream along the Hilbert curve.

5 Conclusion

We have described the form of an optimal solver for lasing systems. This has applications to the ultrafast domain. It may be trivially extended to involve the analysis of high volume experimental data. The methodology described is also applicable to other similar coupled equation solvers and will be quantitatively described in future work. The implementation details involving the optimal message passing and concurrency are ongoing in Rust.

References

[1] J. C. Maxwell, "A dynamical theory of the electromagnetic field," *Philosophical Transactions of the Royal Society of London*, vol. 155, no. 0, pp. 459–512, Jan. 1865. DOI: 10.1098/rstl.1865.0008.

[2] K. Yee, "Numerical solution of initial boundary value problems involving maxwell's equations in isotropic media," *IEEE Transactions on Antennas and Propagation*, vol. 14, no. 3, pp. 302–307, May 1966. DOI: 10.1109/tap.1966.1138693.

[3] S.-H. Chang and A. Taflove, "Finite-difference time-domain model of lasing action in a four-level two-electron atomic system," *Optics Express*, vol. 12, no. 16, p. 3827, 2004. DOI: 10.1364/opex.12.003827.

[4] R. Courant, K. Friedrichs, and H. Lewy, "On the partial difference equations of mathematical physics," *IBM Journal of Research and Development*, vol. 11, no. 2, pp. 215–234, Mar. 1967. DOI: 10.1147/rd.112.0215.

[5] S. C. H. Allen Taflove, *Computational Electrodynamics: The Finite-Difference Time-Domain Method*. ARTECH HOUSE INC, May 11, 2005, 1006 pp., ISBN: 1580538320. [Online]. Available: https://www.ebook.de/de/product/3580196/allen_taflove_susan_c_hagness_computational_electrodynamics_the_finite_difference_time_domain_method.html.

[6] A. C. Polycarpou, "Introduction to the finite element method in electromagnetics," *Synthesis Lectures on Computational Electromagnetics*, vol. 1, no. 1, pp. 1–126, Jan. 2006. DOI: 10.2200/s00019ed1v01y200604cem004.

[7] M. Bader, *Space-Filling Curves*. Springer Berlin Heidelberg, 2013. DOI: 10.1007/978-3-642-31046-1.

[8] A.-J. N. Yzelman and R. H. Bisseling, "A cache-oblivious sparse matrix–vector multiplication scheme based on the hilbert curve," in *Mathematics in Industry*, Springer Berlin Heidelberg, 2012, pp. 627–633. DOI: 10.1007/978-3-642-25100-9_73.